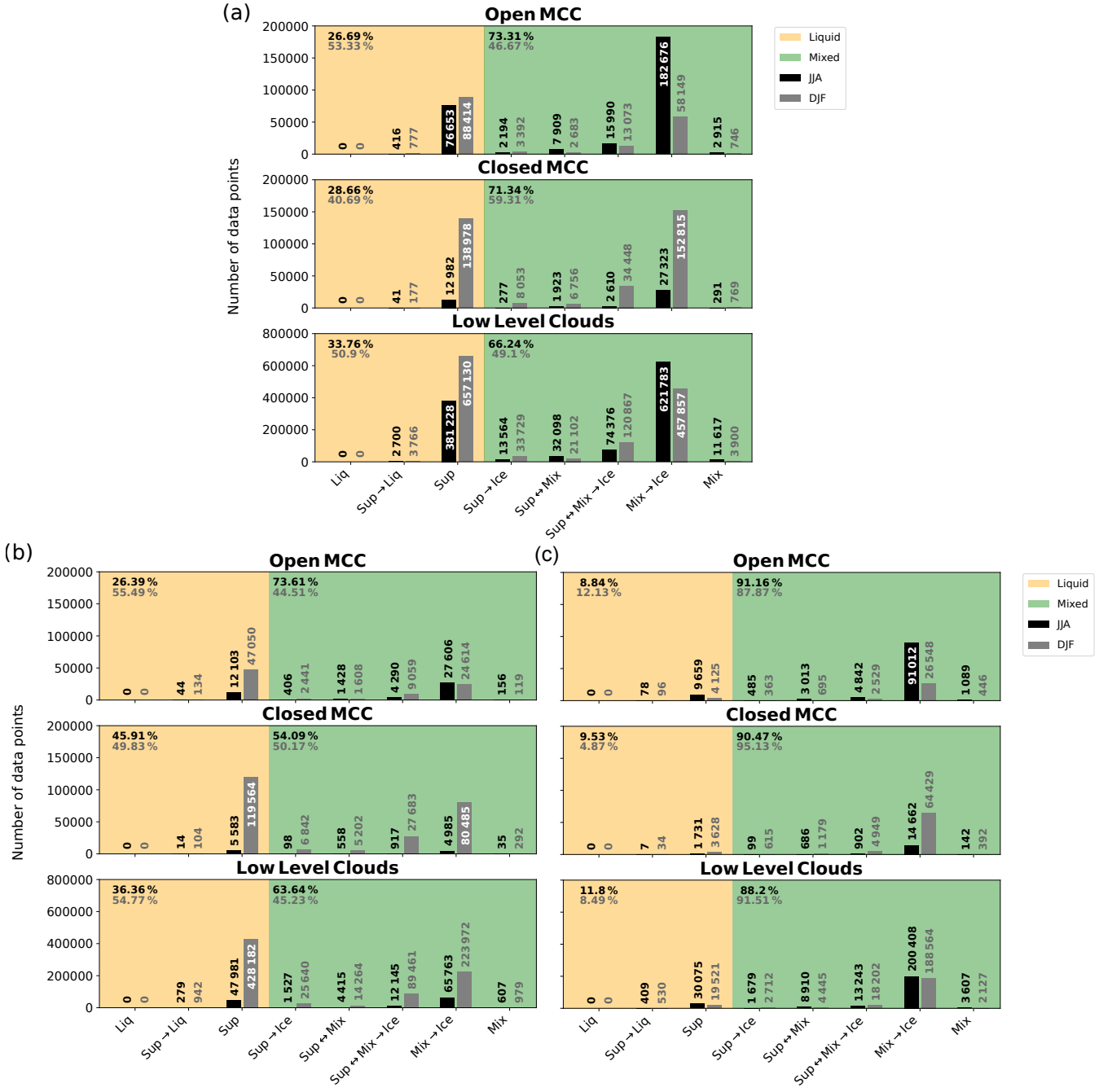

Figure S1. (a) Histogram of data points of vertically resolved cloud phase types divided into two categories: liquid clouds (orange) and MPCs (green) for austral winter (black) and summer (grey) in the temperature range from -20 °C to 0 °C from 2007 to 2010. Overall percentage of liquid clouds and MPCs is indicated in each panel separately for JJA (black) and DJF (grey). "→" indicates layer on top of the next one. "↔" indicates interchangeable layers. (b) Same as (a) but only for clouds with an effective radius $0\,\mu m < R_e < 14\,\mu m$. (c) Same as (a) but only for clouds with an effective radius $R_e > 14\,\mu m$.

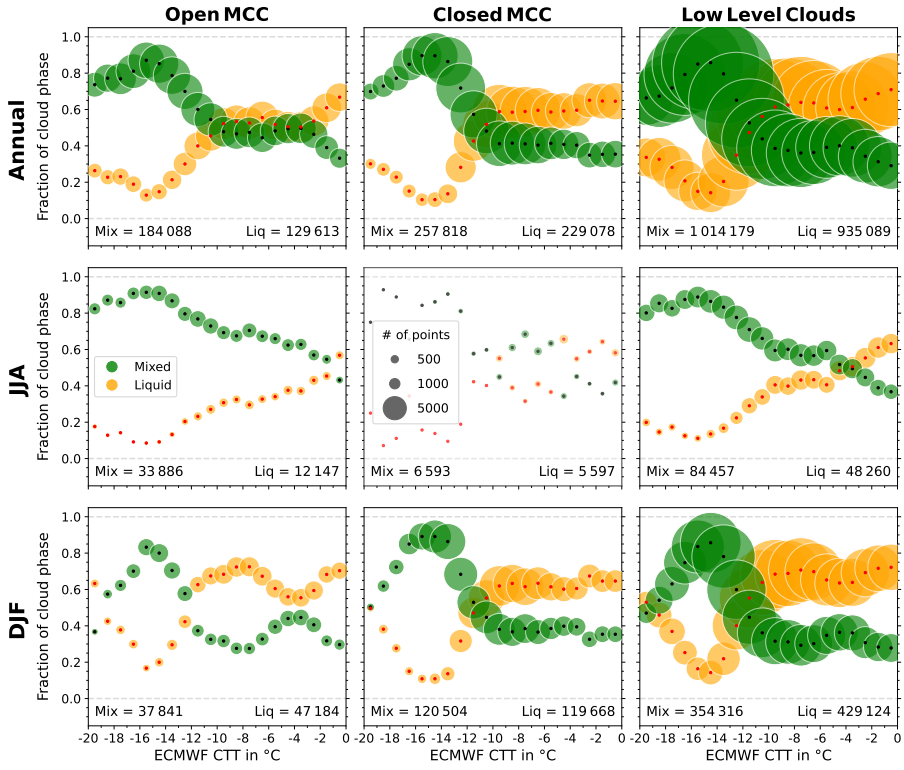

Figure S2. Supercooled liquid and mixed fraction binned by CTT from -20 °C to 0 °C with a bin width of 1 °C (2007 - 2010) for (top) all seasons, (middle) austral winter and (bottom) austral summer in (left) open MCC, (middle) closed MCC, and (right) low level clouds for clouds with an effective radius 0 µm < R_e < 14 µm. As only 5.1 % of the annual closed MCC clouds occur in JJA the panel is displayed in more transparent color shading.

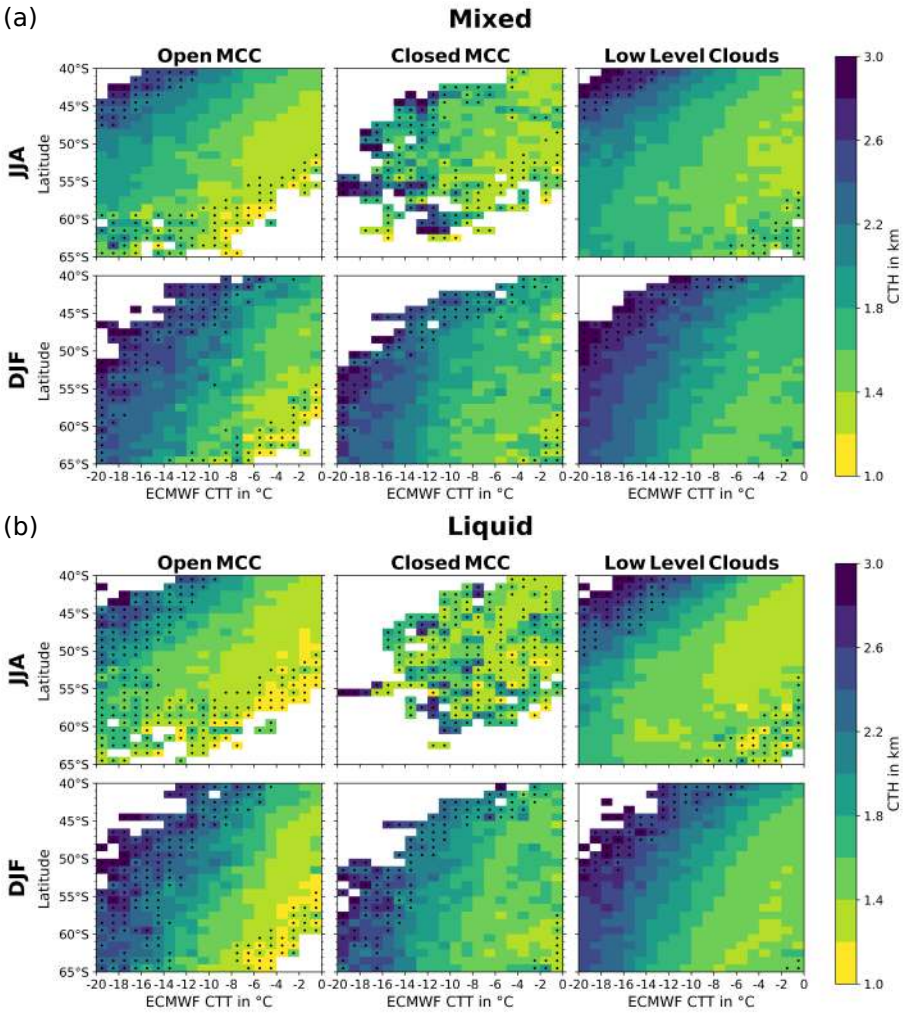

Figure S3. Two-dimensional histograms of CTH against CTT and latitude for (left) open MCC, (middle) closed MCC, and (right) low level clouds in (1. and 3. row) austral winter and (2. and 4. row) summer separately for (a) MPCs and (b) SLCs. Dotted bins indicate bins with less than 50 data points.

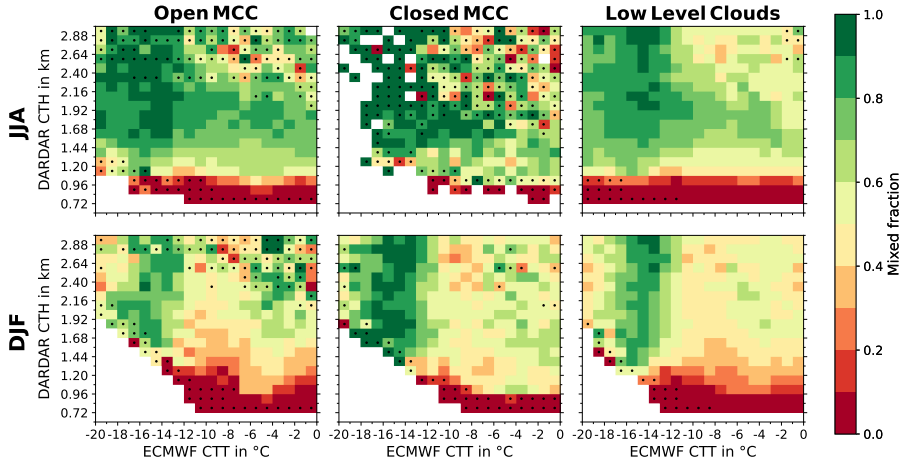

Figure S4. Two-dimensional histograms of mixed fraction against CTT and CTH for (left) open MCC, (middle) closed MCC, and (right) low level clouds in austral (top) winter and (bottom) summer. Dotted bins indicate bins with less than 50 data points.

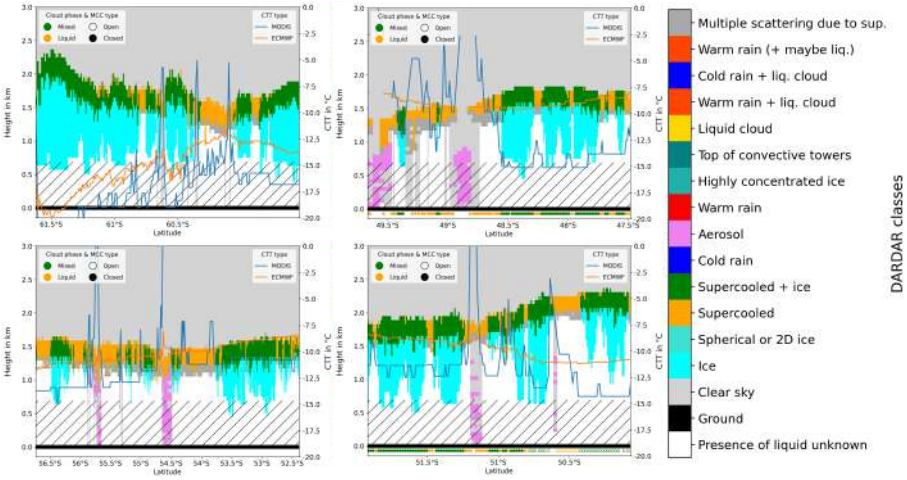

Figure S5. Four example tracks of the DARDAR categorization on 1 December 2007. The blue line indicates the CTT of MODIS and the orange of ECMWF. The hatched area displays levels below 720 m. The colored circles below the ground show the newly defined vertically integrated cloud phase and the MCC type for every other data point.

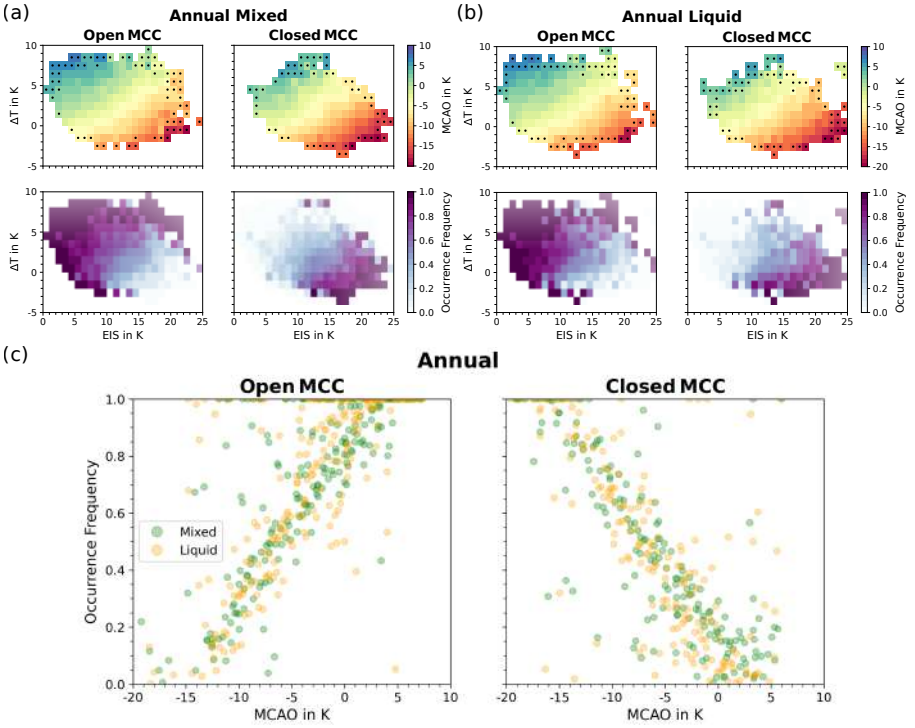

Figure S6. (a) Two-dimensional histograms of (top) the marine cold air outbreak (MCAO) and (bottom) occurrence frequency against ΔT and EIS separately for (left) open MCC and (right) closed MCC MPCs. Dotted bins indicate bins with less than 100 data points. (b) Same as (a) but for SLCs. (c) ΔT–EIS composites computed from the data in (a) for MCPs and (b) for SLCs separated in MPCs and SLCs for (left) open MCC and (right) closed MCC clouds binned by the MCAO index. This figure is produce in a similar way as from Fig. 8 and 9 by McCoy et al. (2017) but separately for MPCs and SLCs. [As MPCs and SLCs occur evenly across the MCAO index, the correlation between ice occurrence and vertical acceleration does not seem to be driven by surface fluxes.]

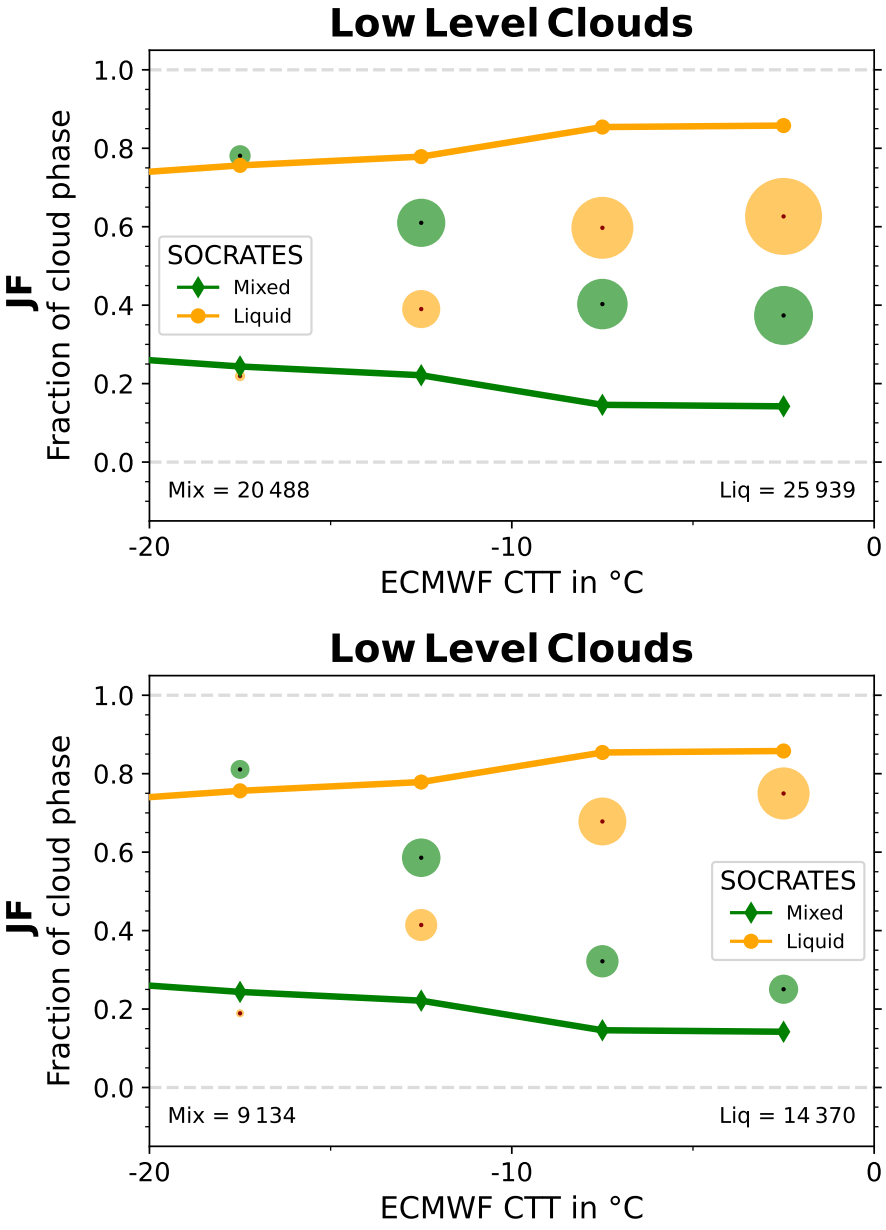

Figure S7. (top) Supercooled liquid and mixed fraction binned by CTT from -20 °C to 0 °C with a bin width of 5 °C (2007 - 2010) for January and February in low level clouds. The months and region (42° S to 62° S and from 133° W to 163° W) are set to match the SOCRATES campaign. SOCRATES data is adapted from Fig. 4 by D'Alessandro et al. (2021). (bottom) Same as top but for only for clouds with an effective radius 0 µm < R_e < 14 µm

References

D'Alessandro, J. J., McFarquhar, G. M., Wu, W., Stith, J. L., Jensen, J. B., and Rauber, R. M.: Characterizing the occurrence and spatial heterogeneity of liquid, ice and mixed phase low-level clouds over the Southern Ocean using in situ observations acquired during SOCRATES, Journal of Geophysical Research: Atmospheres, 126, https://doi.org/10.1029/2020jd034482, 2021.

McCoy, I. L., Wood, R., and Fletcher, J. K.: Identifying Meteorological Controls on Open and Closed Mesoscale Cellular Convection Associated with Marine Cold Air Outbreaks, Journal of Geophysical Research: Atmospheres, 122, 678–11, https://doi.org/10.1002/2017JD027031, 2017.